

Analysis of saturation effects on the operation of magnetic-controlled switcher type FCL

Faramarz Faghihi , Homa Arab

Islamic Azad University South Tehran Branch Young Researchers Club

Keywords: Fault current limiter (FCL), Preisach model , optimization procedure, bias current

Abstract

With the extensive application of electrical power system, suppression of fault current limiter is an important subject that guarantees system security. The superconducting fault current limiters (SFCL) have been expected as a possible type of power apparatus to reduce the fault current in the power system. The results shown that under normal state, the FCL has no obvious effect on the power system; under fault state, the current limiting inductance connected in the bias current will be inserted into the fault circuit to limit the fault current. By regulating the bias current, the FCL voltage loss under normal state and the fault current can be adjusted to prescribed level. This kind of SFCL

used the nonlinear permeability of the magnetic core for create a sufficient impedance and The transient performance considering the magnetic saturation is analyzed by Preisach model.

Preisach model that intrinsically satisfies nonlinear properties is used as the numerical method for analysis of saturation effects. It is able to identification isotropic and no isotropic behaviour. The main idea is to compute the magnetization vector in two steps independently, amplitude and phase. The

described model yield results in qualitative agreement with the experimental results.

1. Introduction

There has been an increase in the number of studies on superconducting fault current limiters (FCLs) to improve the reliability of electrical power systems [1-3] The development of effective FCLs is becoming more and more important in relation to rising fault current levels as more generators and dynamic loads are added to transmission grids.[4] Among the various type SFCL's, the saturated iron core high temperature superconducting FCL (SICSFCL) has many advantages and is more compact in design [5]: it is a rare exception that does not need the quench of superconductivity to create a sufficient impedance for fault current limiting, but by the nonlinear behavior of the magnetic core, which does not have the problem of recovery time [6]. The high temperature superconducting coils are supplied by a dc source and do not have ac power loss. It is thought to be one of the promising candidates for the practical one. However, as mentioned above, the SICSFCL limit the fault current by the nonlinear permeability of the magnetic core, so the ac windings must have a certain number of turns to ensure the sufficiently large

Keywords: magnetic-controlled switcher, fault current limiters, transient analysis

impedance under fault conditions which will result in comparatively large impedance and undesirable voltage loss under normal operation state.

In order to solve this problem, a novel magnetic controlled switcher type fault current limiter topology for high voltage electric network based on the structure of the SICSFCL is proposed. A current limiting inductance is been connected into the bias circuit, and it will be inserted into the ac circuit automatically to limit the fault current when a short circuit fault occurs. In this paper, the current limiting mechanism of the proposed FCL is discussed, and the relationship between magnetic flux density B and magnetic field intensity H discussed by Preisach model. Nonlinear permeability of the magnetic core has very important rule in operation of this fault current limiter. Preisach model gives the exact result for FCL output waves that have the most agreement with the previous presented numerical approaches.

2. Theoretical characteristics of magnetic-controlled switcher type fault current limiter

The topology of the magnetic-controlled switcher type FCL is illustrated in Fig.1. The FCL composed of a magnetic core with three columns which has the effect of magnetic controlled switcher, current limiting inductance and dc bias source. The section area of the yokes and middle column are larger than that of the side columns; the ac windings 1 and 2 are connected in series to a power line, dc bias winding 3 and current limiting inductance is connected into the dc circuit. three-phase full-bridge controlled rectifier provides dc bias current for the FCL. Under normal operation state, the dc bias current is adjusted to make the side columns core in deep saturated state, while the yokes and the middle column core are in unsaturated state due to the larger section area than the side columns.

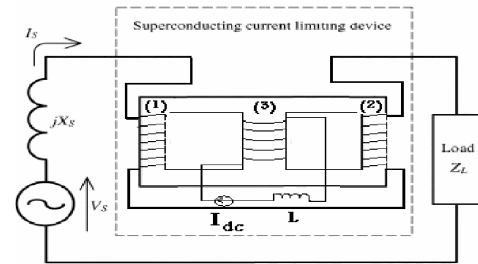


Fig.1 . Topology of the magnetic controlled switcher type fault current limiter.

Under normal state, the magnetic-controlled switcher is turned off, the current limiting inductance has no obvious effect on the ac circuit, the impedance of the FCL is very low and the voltage drops on the ac windings are low. When a fault occurs, the amplitude of the fault current is increased and generates an ac magnetic motive force (mmf) large enough to counteract the dc bias mmf and desaturated the side columns core. In the negative half cycle of the ac current, the right side column will be desaturated, the FCL works like a single phase transformer, the right side winding as the primary winding and the bias winding as the secondary winding, the magnetic-controlled switcher is turned on, the current limiting inductance L will be converted into the ac circuit to limit the fault current automatically. At the same time, the ac mmf in the left side column is in the same direction with the dc bias mmf, the left side column will be in deeper saturate state and has no effect on the fault current.

Two side columns are used here for the fault current limitation in positive and negative half cycle of the ac current alternatively. The section area of the yokes and middle column are larger than that of the side columns, this kind of design has two advantages: one is that the side columns can be easily be driven into saturation by the bias current while the middle column and the yokes are in unsaturated state; the other is that when the side columns are been desaturated after the fault, it will be work as a single phase transformer with the middle column immediately, the magnetic controlled

Switcher switches on and the current limiting inductance L will be connected into the ac circuit to limit the fault current.

3. Bias current influence on the FCL voltage loss under normal state

The bias current plays a very important role in the magnetic-controlled switcher type FCL operation. Under normal operation state, the bias current must provide a dc mmf large enough to saturate the side columns core; under fault state, the magnitude of bias current determines the period of time when the current limiting inductance be converted into the fault circuit, thus determines the magnitude and form of the limited current. The bias current influence on the characteristic of the FCL will be analyzed in the following paragraphs. Template Suppose the bias current is i_{dc} , then the bias mmf can be written as

$$F_{dc} = i_{dc} N_{dc} \quad (1)$$

where, N_{dc} is the turn of bias winding. The bias magnetic field intensity is

$$H_0 = F_{dc} / l \quad (2)$$

Where, l is the mean length of magnetic circuit. Then the bias magnetic flux density can be written as

$$B_0 = f(H_0) \quad (3)$$

Where in equation (3), f is the function expressing the relationship between magnetic flux density B and magnetic field intensity H . Preisach model is used for identification this function.

3. Using of Preisach model for studying of saturation effect in magnetic-controlled switcher type

The model introduced in this section fits in the category of vector Preisach coupled-hysteron models. The magnetization is computed in two steps, first the amplitude and second the angle between vector magnetization and vector applied field ($\phi = \theta - \alpha$ see Fig.2). This model in two dimensions is defined by means of the following terms: two Preisach independent functions computed in the principal axes of the system (easy $P_x(U_x, V_x)$ and hard $P_y(U_y, V_y)$), a

weight function $G(a)$, a phase diagram composed by a boundary function $L_\phi(\alpha, |H|)$, and a history function $T(\Delta\alpha)$ (α is the angle between vector applied field and vector magnetization). The hysteron coupling is obtained by means of both weight function and phase diagram. This model satisfies both saturation and loss properties intrinsically.

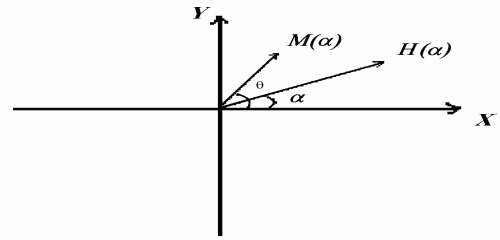


Fig 2. Applied field and magnetization for fixed α

The identification of the model parameters can be solved by means of a reduced set of experimental data, which includes both rotational and alternating loops. A key point of a simple identification procedure described below is to postulate that the vector magnetization is oriented in the same direction of vector applied field when the starting magnetic state is the demagnetizing one and an alternative field is applied. So, the $P_x(U_x, V_x)$ function can be computed by the knowledge either of first-order reversal curves [8] or of a set of symmetric minor loops [9], as in scalar hysteresis identification. In analogy for the $P_y(U_y, V_y)$ computation. For a fixed direction α of applied field vector, the Preisach function is given by :

$$P_\alpha(U_\alpha, V_\alpha) = (1 - G(\alpha))P_x(U_x, V_x) + G(\alpha)P_y(U_y, V_y) \quad (4)$$

Where $G(a)$ has magnitude between 0 and 1. For a generic history of the applied field, the magnetization is computed solving the double Everett integral [6].

$$M(H(\alpha, t)) = \iint_{D^+} P_\alpha(U_\alpha, V_\alpha) dU_\alpha dV_\alpha - \iint_{D^-} P_\alpha(U_\alpha, V_\alpha) dU_\alpha dV_\alpha \quad (5)$$

Where $M(H(\alpha, t))$ and $H(\alpha, t)$ are the input and the output of the model at the time t . D^+ and D^- are the positive and negative domain of Preisach triangle where the hysterons give a

positive or a negative contribution to the total magnetization.

The maximum value of the magnetization predicted by (2) can achieve the saturation magnetization M_s . When the magnetic material behaviour is isotropic, for each direction $P_\alpha(U_\alpha, V_\alpha) = P_x(U_x, V_x)$; otherwise, the weight function $G(\alpha)$ is determined by fitting the Preisach function computed by means of measurements of alternative applied field along different α -directions. The Preisach functions have to satisfy the symmetry property : $P_\alpha = P_{-\alpha} = P_{\pi-\alpha} = P_{\pi+\alpha}$, this means that : $G(a) = G(-a) = G(\pi - \alpha) = G(\pi + \alpha)$. A generalization of the model and in particular of the (1) includes the $P_\alpha(U_\alpha, V_\alpha)$, computation as follows :

$$P_\alpha(U_\alpha, V_\alpha) = F(P_x(U_x, V_x), P_y(U_y, V_y), \alpha) \quad (7)$$

Where F (Which can be identified by experimental alternative data) satisfies the following properties:

$$\begin{cases} P_x(U_x, V_x) = F(P_x(U_x, V_x), P_y(U_y, V_y), 0) \\ P_y(U_y, V_y) = F(P_x(U_x, V_x), P_y(U_y, V_y), \pi/2) \end{cases} \quad (8)$$

The two Preisach functions P_x and P_y are both located in the same Preisach plane. The applied vector Field $H = H(\alpha)$ is separated two vectors, $H_A = [H_1, \dots, H_N]$ which gives the magnitude and $\alpha = [\alpha_1, \dots, \alpha_N]$ which gives the angle between vector field and x-axis. Using the first, we solve the Everett integrals in the same Preisach plane but with P_x and P_y as Preisach function, obtaining two values, of magnetization (M_x, M_y) for each element of the vector. By the knowledge of the second vector we compute the values of the weight function G and the final value of the magnitude of magnetization as $M_t = (1 - G(\alpha))M_x + G(\alpha)M_y$.

From the computational point of view the magnitude computation in this model is the larger time consuming step, but is about two times the CPU times for a scalar approach such as the CSPM.

The Φ angle between magnetization and applied field depends on the magnitude of the applied field, on the angle between vector applied field and a fixed direction, and on the

magnetic history. We introduce a phase diagram that takes into account all of these aspects, we postulate only that there is a lag angle between the vector applied field and the vector magnetization, this is verified experimentally in most cases.

The phase diagram can be computed in two steps: the boundary $L_\phi(\alpha, |H|)$ and the $T(\Delta\alpha)$. The former can be computed by means of the knowledge of the experimental rotational loops and it is implemented in numerical way. The magnitude of the applied field (from zero to saturation field H_s) is divided in $N+1$ point, $H = [0, \Delta H, 2\Delta H, \dots, N\Delta H]$, being $N\Delta H = H_s$. Experimentally, the measurements start by the saturate rotational loop ($|H| = H_s$) Where the field and the magnetization are parallel, decreasing for each measurement step the field magnitude of ΔH we obtain by the rotational loop the angle between vector magnetization and vector applied field as function of α in particular the value of the angle is max for $\alpha = 0$ and it decrees until a minimum at $\alpha = \pi/2$. All of these give the whole phase diagram boundary $L_\phi(\alpha, |H|)$. The phase diagram can be computed also using the rotational loop measured for constant magnitude of magnetization $L'_\phi(\alpha, |M|)$.

Its computation can be done likewise to the $L_\phi(\alpha, |H|)$ but considering a vector of $|M| = [0, \Delta M, 2\Delta M, \dots, N\Delta M]$. It can be proved that $L'_\phi(\alpha, |M|)$ and $L_\phi(\alpha, |H|)$ are equivalent.

We draw attention to an important aspect, $H = H_s$ the phase diagram boundary is reduced to a point. This gives magnetization and applied field parallel at saturation field, this fact gives the rotational losses zero at saturation yielding the loss property intrinsically.

The identification of function $T(\Delta\alpha)$ is nontrivial and the knowledge of alternative and rotational loop is not enough to solve it, the complete identification procedure will be discuss elsewhere. However, in order to reproduce alternative and rotational loops and losses, the knowledge of $T(\Delta\alpha)$ is not necessary.

In the theoretical case of isotropic material, namely the physical behaviour is the same for each direction. For a rotational loop related to a value of magnitude of magnetization or field, the angle between the magnetization and the applied field depends on the amplitude itself [8]-[9] only, so the phase diagram boundary becomes a function of the magnetization $L'_\varphi(H)$ only.

4. transient analysis of transformer type SFCL

The schematic diagram used for transient analysis shown in Fig.3.

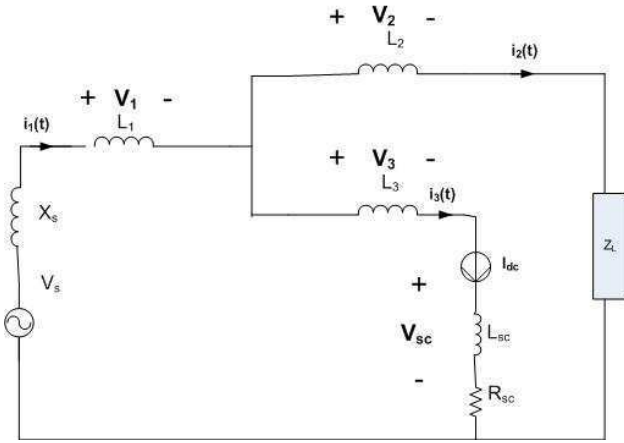


Fig. 3 . equivalent circuit used for transient analysis.

By using this schematic diagram, the equations of voltage are given as follows.

$$V_1(t) = L_{11} \frac{di_1(t)}{dt} + R_1 i_1(t) + L_{12} \frac{di_2(t)}{dt} + L_{13} \frac{di_3(t)}{dt} \quad (9)$$

$$V_2(t) = L_{21} \frac{di_1(t)}{dt} + L_{22} \frac{di_2(t)}{dt} + R_2 i_2(t) + L_{23} \frac{di_3(t)}{dt} \quad (10)$$

$$V_3(t) = L_{31} \frac{di_1(t)}{dt} + L_{32} \frac{di_2(t)}{dt} + R_3 i_3(t) + L_{33} \frac{di_3(t)}{dt} \quad (11)$$

$$V_3(t) = L_{sc} \frac{di_3(t)}{dt} + R_{sc}(t) i_3(t) \quad (12)$$

L_{sc} is residual inductance of the super conducting current limiting device, which is equal to 28 mH. It is measured experimentally under a variety of fault condition.

In normal condition, resistive type SFCL is zero. If path current through the SFCL is more than its circuit current, R_{sc} can be represented by the following expression.

$$R_{sc} = R \left[1 - \exp\left(-\frac{t-t_q}{\tau}\right) \right] \quad (13)$$

where R is the maximum value of the current limiting device resistance, and τ is the time constant of the resistance increase. Moreover, $t=0$ is the time when the transmission line fault occurs, and $t=t_q(>0)$ is the time when the S-N transition starts.

The magnetizing current $i_3(t)$ is expressed by considering the magnomotive force and By combining equation (15) and (20) we can obtain that

$$\varphi = \left(\frac{NA}{l\bar{\mu}} \right) i_3(t) \quad (14)$$

$\bar{\mu}$ can be achieved from equations (2) up to (8).

By using (9)-(13) and (14), the transient waveforms of the transformer type SFCL can be calculated.

5. Result and discussions

As shown in Fig 4, 5, when the bias current is small, the SFCL voltage is very high for the side columns core has not been saturated by the bias current, the FCL impedance is large and the voltage lost can not be neglected. With the increase of the bias current, the bias mmf drives the side columns core in saturation and the FCL impedance becomes low, so does the FCL voltage.

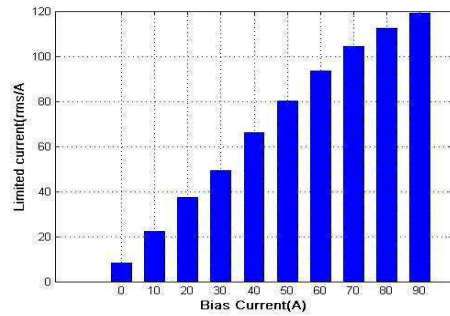


Fig 4. Relation between limited currnt and bias current

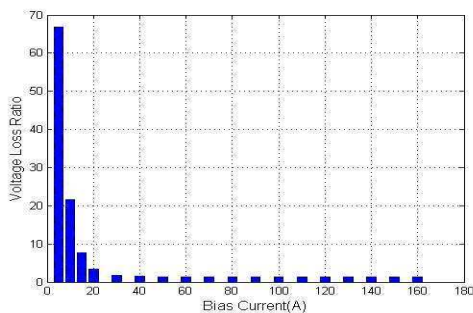


Fig 5. Relation between Bias Current and Voltage Loss Ratio

Fig 6, 7 demonstrate the fault current limiting effect and examine the relationship between the bias current and the limited fault current, hence as to determine the bias current by the requirement of preset fault respectively.

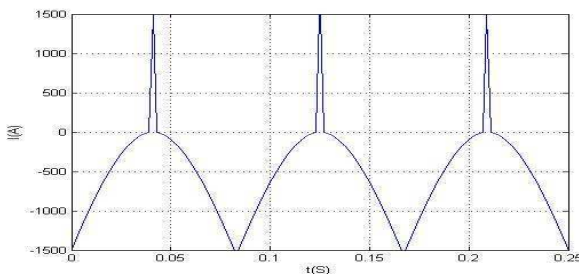


Fig 6. Short Circuit fault current without FCL

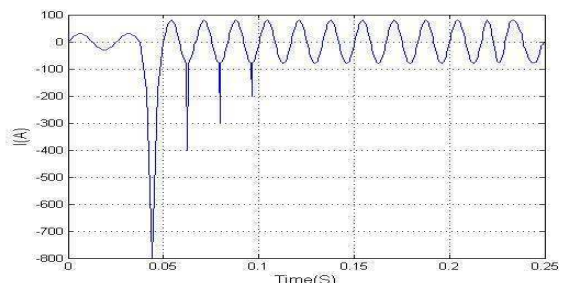


Fig 7. Short Circuit fault current with FCL

The fault current wave form with FCL is shown in Fig. 7 when the bias current is 50A and without FCL is shown in Fig. 6. Comparing the fault current with and without the FCL, the amplitude of the Fault current was reduced by about 50% in this model.

The calculated Waveform based on suggested model is very close to those obtained from Froehlich Formula [10].

6. Conclusion

Effects of $B-H$ curve on the operation of transformer type SFCL is very crucial. In this

paper, a novel optimized procedure for modeling of magnetic saturation effects was proposed. Preisach model gives the exact result for FCL output waves that have the most agreement with the previous presented numerical approaches such as Froehlich formula. The results of this analysis are very useful for quantitative estimation and have to be considered in the design of magnetic controlled switcher type fault current limiter.

References

- [1] Muta, I. Doshita, T. Nakamura, T. Egi, T. Hoshino, T. Dept. of Electr. Eng., Kyoto Univ., Japan; "Influences of superconducting fault current limiter (SFCL) on superconducting generator in one-machine double-line system," *IEEE Trans. Appl. Supercond*, Vol. 13, NO.2, June 2003.
- [2] I. Muta, T. Doshita, T. Nakamura, T. Egi, T. Hoshino, "Influences of superconducting fault current limiter (SFCL) on superconducting generator in one-machine double-line system," *IEEE Trans. Appl. Supercond*, Vol. 13, Issue 2, June 2003.
- [3] H. Yamaguchi, T. Kataoka, "Comparative Study of Transformer-Type Superconducting Fault Current Limiters Considering Magnetic Saturation of Iron Core," *IEEE Trans. Appl. Supercond*, Vol. 42, Issue 10, Oct. 2006.
- [4] S.-H. Lim, H.-S. Choi, D.-C. Chung, Y.-H. Han, "Fault current limiting characteristics of resistive type SFCL using a transformer," *IEEE Trans. Appl. Supercond*, Vol. 15, NO.2, Jun. 2005.
- [5] A. Reimers, M. Gyimesi, E. Della Torre, D. Ostergaard, "Implementation of the Preisach DOK magnetic hysteresis model in commercial finite element package," *Magnetics, IEEE Trans*, Vol 37, Issue 5, Sep 2001.
- [6] E. Della Torre, *Magnetic Hysteresis*. Piscataway, NJ: IEEE Press, 2000.
- [7] Endo, H.; Hayano, S.; Saito, Y., "An image-based approach for Preisach function calculation" *IEEE Trans* Vol 38, Issue 5, Sep 2002.
- [8] I. D. Mayergoyz, *Mathematical models of Hysteresis*. New York: Springer-Verlag, 1991.
- [9] B. Azzzerboni et al, "A comparative study of Preisach scalar hysteresis models," *Physica B*, Vol. 343, pp. 1-9, 2004.
- [10] H. Yamaguchi, T. Kataoka, "Effect of magnetic saturation on the current limiting characteristics of Transformer-Type Superconducting Fault Current Limiters," *IEEE Trans. Appl. Supercond*, Vol. 16, NO. 2, June 2006.